Proc. of the 30th International Slovak–Polish Scientific Conference on Machine Modelling and Simulations 2025

Modelling of Mechanical Properties of Thermoplastic Elastomer for Simulation of Belt Welding Process

K. Wałęsa*, K. Talaśka and D. Wilczyński

Institute of Machine Design, Faculty of Mechanical Engineering, Poznan University of Technology, Piotrowo 3, 61-138 Poznań, Poland

Doi: 10.12693/APhysPolA.149.S68 *e-mail: krzysztof.walesa@put.poznan.pl

Hot plate welding is a popular method for butt joining drive and conveyor belts made of thermoplastic elastomers. A crucial step in this technological operation is the plasticisation of the belt material on a hot plate, which occurs under the influence of locally elevated temperature and the action of axial compressive force. Due to the multiplicity of parameters in the plasticisation process, there are opportunities for its optimisation, mainly in terms of energy efficiency. Such an action can positively impact the energy consumption of the welding operation, and, thus, the entire belt manufacturing process. The paper presents the results of numerical and experimental studies on the modelling of the mechanical properties of a polyurethane-based thermoplastic elastomer used in the manufacture of belts. In the first stage of the experimental studies, the stress response of the material to displacement was determined based on the results of a static tensile test. The obtained stress–strain characteristics were used to perform numerical tests using the finite element method. In this stage of the work, various types of hyperelastic material models, including Mooney–Rivlin, Ogden, Neo-Hooke, Yeoh, Arruda–Boyce, and Marlow, were used to map the static tensile test in the simulation. Based on the assessment of the convergence of numerical and experimental results, three hyperelastic models were selected that could be used to model the properties of this material; these were the second-order polynomial, the third-order Ogden, and the fourth-order Ogden. Additionally, based on observations from the first stage of experimental and numerical studies, it was determined that modelling the mechanical deformation process of this belt may require the use of a material model that takes into account the deformation speed. These observations were confirmed during the second stage of experimental research, where a static tensile test showed the effect of strain rate on the stress–strain characteristics, which may suggest the need to refine the hyperelastic model by incorporating viscoelasticity. The results and conclusions from the physical tests will be used to further refine the numerical model, which will be used during the optimisation of the belt plasticising operation.

topics: welding, thermoplastic elastomer, hyperelasticity, viscoelasticity

1. Introduction

Pressure welding is a popular method for making permanent joints in machine [1] and vehicle [2] design and is used to join metallic and non-metallic materials, including polymers [3]. Permanent joints of polymer materials can also be made in different ways, including bonding, welding, or using other types of mechanical fasteners that prevent the joint from being separated without destroying the joined elements or the fastener [4]. One of the most popular methods of welding plastics is butt welding using a hot plate, which is used in the production processes of various plastic products [5]. This method of making permanent joints is also used in the production of circular cross-section drive and conveyor belts made of thermoplastic elastomers [6]. The authors are conducting research and development work on this process, the main goal of which is to automate the welding of such belts.

Many researchers have addressed various aspects of butt welding of polymer materials in their work. The results they presented most often included experimental determination of the strength of the weld, as well as its correlation with the technological parameters of welding, in particular: pressure force, hot plate temperature, and the duration of individual phases of the process [7, 8]. The literature also includes works on modelling [9] and optimisation of this process [10]. The results of the cited research are interesting in that they allow for a general assessment of the impact of individual welding parameters on the outcome of this process. However, in all these cases, scientists have been studying the welding of materials with relatively high stiffness, rather than materials as flexible as the thermoplastic elastomer from which the belts are made. There are also many works in the literature concerning the modelling of the properties of elastomers as hyperelastic materials. Qi et al. [11] addressed the topic of stress–strain correlation for thermoplastic polyurethane.

In his work, he developed the parameters of the constitutive model of this material based on observations made during experimental studies of cyclic deformation. Drozdov et al. [12] undertook the development of a constitutive model of an ethylene-based thermoplastic elastomer under standard environmental conditions. For this purpose, tests were carried out under triaxial loading conditions, which allowed for the determination of the elastic and viscous responses to displacement loading. Labmert-Diani et al. [13] analysed the elastic deformation energy for a hyperelastic elastomeric material and rubber in their work, without specifying precisely which material was tested. Based on uniaxial tensile, pure shear, and biaxial tensile tests, as well as analytical operations on elastic deformation energy functions, a strategy was developed to determine the material's response to displacement.

There are also many publications on the numerical modelling of hyperelastic materials, including thermoplastic elastomers. Eberlein et al. [14] analysed the use of linear viscoelastic and non-linear viscoelastic-plastic models in modelling the penetration of a thermoplastic polyurethane (TPU) sample by a metal conical blade. The conclusions from the work indicate that large deformations of this type of material, combined with its destruction, require consideration of the material's non-linearity and plasticity. The authors also presented their own method of calibrating the material model, taking these characteristics into account. That work is a source of valuable information for modelling the properties of polymer materials, but the results themselves, due to the different way of sample loading, are not useful for the analysis of a welded belt. Wojnowski et al. [15], in turn, presented an overview of the knowledge on modelling elastic deformations in thermoplastic elastomers, in particular in materials based on polyethylene terephthalate, using the Mooney–Rivlin (M-R) model. In their experimental and numerical studies, the authors showed that it is not possible to use a simple M-R model (described by two basic coefficients) to evaluate the response of the studied material to cyclic displacement loading, because this model does not reflect the phenomena associated with creep and relaxation of the material. Wang's work [16] appears to be a comprehensive review of the state of knowledge on modelling the hyperelastic properties of polyurethane-based thermoplastic elastomers and the preparation of a numerical model for simulating the stretching process. The methodology proposed in this paper is noteworthy; however, in the case of the belt material, it is first necessary to assess which of the hyperelastic material models will properly reflect the characteristics obtained from the experimental studies, as the research presented by the authors focuses exclusively on the generalised Mooney–Rivlin model.

As evidenced by a review of the literature, many researchers have addressed the topic of butt welding of plastics. Numerous studies have also been conducted on modelling the properties of plastics, particularly elastomers, including thermoplastics. However, it is difficult to find examples in the literature of work involving the modelling of the properties of a specific product made of polyurethane-based thermoplastic elastomer — belts used in drive systems or conveyors. There is even less information on the development of numerical models for this type of product. The available technical information on the properties of this material is also very general. These factors lead the authors to identify a research gap related to this topic. Therefore, steps have been taken to facilitate further research on butt welding of belts, in particular the analysis and optimisation of the individual phases of this technological process. The authors decided to start numerical research, including testing the response of the belt material to mechanical stress. In the initial phase of these activities, it was planned to develop a numerical model to simulate the deformation of the belt material under uniaxial loading in standard environmental conditions (i.e., at a constant temperature of $\approx 20°C$). Due to the fact that a uniaxial load state occurs during the individual phases of the welding process, it was decided to focus only on this type of interaction. Therefore, the results of a static tensile test, which was reproduced in a numerical simulation, were used for the research.

2. Materials and methods

The material tested was a thermoplastic elastomer based on polyurethane TPU C 85 A, which is used to manufacture flat and circular belts subjected to the welding process tested by the authors [17]. The tests presented in this article were performed only on samples taken from flat belts with a thickness of 4 mm and a width of 140 mm. It should be noted that in previous studies, the authors demonstrated that for the purposes of analysing the welding process of a belt made of TPU C 85 A, it is possible to use samples taken from flat belts and belts with a circular cross-section interchangeably [18].

For the experimental studies, paddle samples (cut from a flat belt with a die cutter) were used, with dimensions compliant with ISO 527-2 [19]. Two sample sizes were used in the experimental tests, namely large 1B-type fittings (in preliminary experimental tests and numerical tests) and 1BA-type fittings (in the second part of the experimental tests). The reduction in sample size in the second part of the experimental tests was due to the limited availability of material for testing. Samples were tested at a constant temperature ($\approx 20°C$).

The first part of the experimental research, the results of which were used to formulate the general numerical model, was carried out at earlier stages of the research work for the purpose of identifying

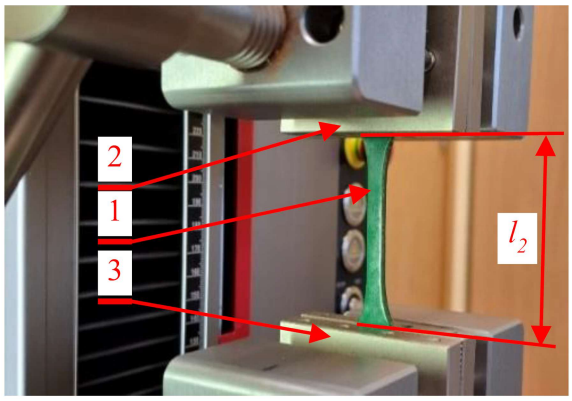

Fig. 1. Fixing a type 1BA paddle specimen in the grips of a ZwickRoell Z5.0 TN zwickiLine testing machine: 1 — specimen, 2 — movable crosshead grip, 3 — fixed grip, l_2 — initial distance between the grips.

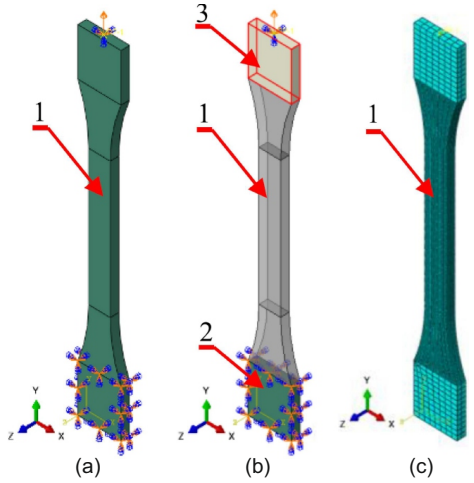

Fig. 2. Geometrical models used in the numerical simulations: (a) general model of the test sample (1), (b) model with applied boundary conditions, (c) model with imposed finite element mesh. Notation: 1 — sample, 2 — fixed surface, 3 — surface with imposed displacement boundary condition.

the mechanical properties of this material. The test parameters were as follows [20]:

- constant test speed $v_t = 60$ mm/min;
- limit of deformation $\varepsilon_{t\_\max} = 3$;
- MTS Insight 50 kN testing machine.

The test parameters for the second part of the experimental tests were as follows:

- different test speeds $v_t = 10$, 20, 50, 100, 200, 300, and 500 mm/min [21];
- limit of deformation $\varepsilon_{t\_\max} = 3$;
- ZwickRoell Z5.0 TN testing machine.

In both cases, the force was measured using a force sensor placed on the movable crosshead of the testing machine, while the displacement was recorded using a crosshead position sensor. The relative deformation of the material during the test was determined based on the following correlation

$$\varepsilon_t = \frac{\Delta l_2(t)}{l_2}, \tag{1}$$

where ε_t is the current deformation; l_2 — measured length resulting from the initial distance between parallel parts of the sample, resulting from normative guidelines for both types of samples [19]; Δl_2 — change in the measured length occurring during the test. The samples in the grips of the testing machine were mounted in such a way that the edge of the grips was aligned with the end of the parallel parts of the sample, i.e., the initial distance between the machine grips was l_2 (Fig. 1).

Numerical studies were conducted in the Abaqus 2024 system using the static analysis module following the Implicit procedure. The aim of the research was to obtain the parameters of a hyperelastic model, which was supposed to allow for the reproduction of the material's response to displacement forces during stretching of a paddle specimen in a static tensile test. In the first stage, after launching the calculation procedure enabling the use of the hyperelastic model, test data — results of the static tensile test performed in the first stage of the experimental research — were implemented into the Abaqus software. On this basis, the suitability of standard hyperelastic material models for simulating the experiment was assessed. This assessment was made by checking the stability of the calculations for individual model types and load types. On this basis, it was also possible to obtain the parameters of individual models. In the second stage, after preliminary verification of the available models and obtaining their parameters, finite element method (FEM) simulations of the static tensile test were performed in order to finally verify which models reproduce this process with sufficient accuracy. The configurations of the test samples subjected to testing are shown in Fig. 2 (these models were prepared in Abaqus software). The assumptions regarding boundary conditions and numerical test parameters were as follows:

- the sample (marked by "1" in Fig. 2a) with a paddle shape of type 1B and dimensions compliant with standard ISO 527-2 [19] was used;
- the sample was mounted on surfaces 2, and a displacement condition was applied with a speed of $v_t = 60$ mm/min on surfaces 3, in the direction of the Y-axis, until the deformation value of the measuring part was obtained, i.e., $\varepsilon_{t\_\max} = 3$ (for experimental tests, this was the part between the grips of the testing machine with a length of l_2; see Fig. 1);

- a C3D8R finite element mesh was used, with an average element size of 2 mm, with a 4-fold densification in the Y-axis direction, along the entire length of the measuring part (l_2 in Fig. 1);
- the results were obtained by reading the displacement of a reference point located in the grip part of the sample (associated with surfaces 3; see Fig. 2b) and the concentrated force recorded at this point. This allowed for the measurement conditions on the testing machine to be reproduced.

3. Results and discussion

When modelling the hyperelastic properties of materials, instead of classic parameters such as Young's modulus or Poisson's ratio, the strain energy density function is often used to describe mechanical properties. Its general form is [16]

$$W = W(I_1, I_2, I_3), \tag{2}$$

$$I_1 = \lambda_1^2 + \lambda_2^2 + \lambda_3^2, \tag{3}$$

$$I_2 = (\lambda_1 \lambda_2)^2 + (\lambda_2 \lambda_3)^2 + (\lambda_3 \lambda_1)^2, \tag{4}$$

$$I_3 = (\lambda_1 \lambda_2 \lambda_3)^2, \tag{5}$$

where I_1, I_2, and I_3 are the invariants of the Cauchy–Green deformation tensor, and λ_1, λ_2, and λ_3 are the deformation indices in different directions. This is a very general constitutive model of a hyperelastic material. In practice, this description is refined by using various models that are specific forms of this equation. These models can be developed on the basis of continuum mechanics, such as polynomial (including Mooney–Rivlin), reduced polynomial (including Neo-Hooke and Yeoh), and Ogden's model, or on the basis of thermodynamics principles — models such as Arruda–Boyce, Van der Waals, and Marlow [16, 22].

In the first stage of numerical research, computational stability was demonstrated by: polynomial models of the 1st and 2nd order (including Mooney–Rivlin), Ogden models (1st to 4th order), reduced polynomial models (1st, 3rd, and 5th order — including Neo-Hooke and Yeoh), and Arruda–Boyce and Marlow models. The other models did not show computational stability at all or did not show it for deformations greater than a specified value. As a result, these models did not meet the input conditions for the research. Based on this evaluation procedure, the parameters of each model were also determined (we used them in the next part of the numerical research). During this part, a comparative analysis of the response of the paddle sample to displacement excitation was performed with the experimental results obtained in the first stage of the experimental research. The numerical tests used the aforementioned material models, which showed computational stability over the entire range of specified deformation ($\varepsilon_{t\_\max} = 3$). The obtained characteristics are presented in Fig. 3.

As can be seen from the obtained characteristics (Fig. 3a–d), some models of hyperelastic material did not allow for obtaining results in the entire range of the deformation; the analysis did not achieve computational convergence after exceeding a certain value of this parameter. These models: Yeoh (Yeoh), reduced 5th order polynomial (redPoly5), Marlow (Mar), and 1st order Ogden (Og1), will not be considered in further discussions. The remaining cases allowed for convergence of calculations across the entire range of deformation, as evidenced by the fact that the numerical simulation was successful until the end. When assessing the fit of the obtained characteristics to the results of experimental studies, it should be noted that:

- the Mooney–Rivlin (M-R), Ogden 2nd order (Og2), Neo-Hooke (N-H), and Arruda–Boyce material models (respectively in Fig. 3a–d) do not accurately reproduce the experimental results. The characteristics obtained using these models differ in form from the experimental results. This indicates that these models do not accurately reflect the actual response of this material during a static tensile test. Therefore, at this stage, they have been rejected from further analysis;
- material models (respectively in Fig. 3a–b), i.e., 2nd order polynomial (Poly2), 3rd and 4th order Ogden (Og3 and Og4), reproduce the shape of the static tensile test result obtained in experimental tests quite well. However, a difference was noted between the individual tensile stress values from the experiment σ_{t_exp} and the values obtained from the numerical simulation σ_{t_fem} in almost the entire deformation domain ε_t.

For the purposes of analysing this phenomenon, the percentage difference between the experimental and numerical results was calculated. In order to standardise the domain of the $\sigma_t(\varepsilon_t)$ function for both cases, the obtained characteristics were approximated using a 6th degree polynomial function, with the mathematical model fitted to the data, expressed by the coefficient of determination $R^2 > 0.997$. Then, on this basis, the percentage difference $\Delta\sigma_{t\_exp\_fem}$ between the experimental results σ_{t_exp} and numerical results σ_{t_fem} was determined using

$$\Delta\sigma_{t\_exp} = \frac{\sigma_{t\_exp} - \sigma_{t\_exp\_fem}}{\sigma_{t\_exp}} \times 100\%. \tag{6}$$

The function of this indicator in the ε_t deformation range is plotted in Fig. 3e; the determined percentage difference is approximately 11% at most, and only in the range of deformation values exceeding 150%. This indicates that the numerical

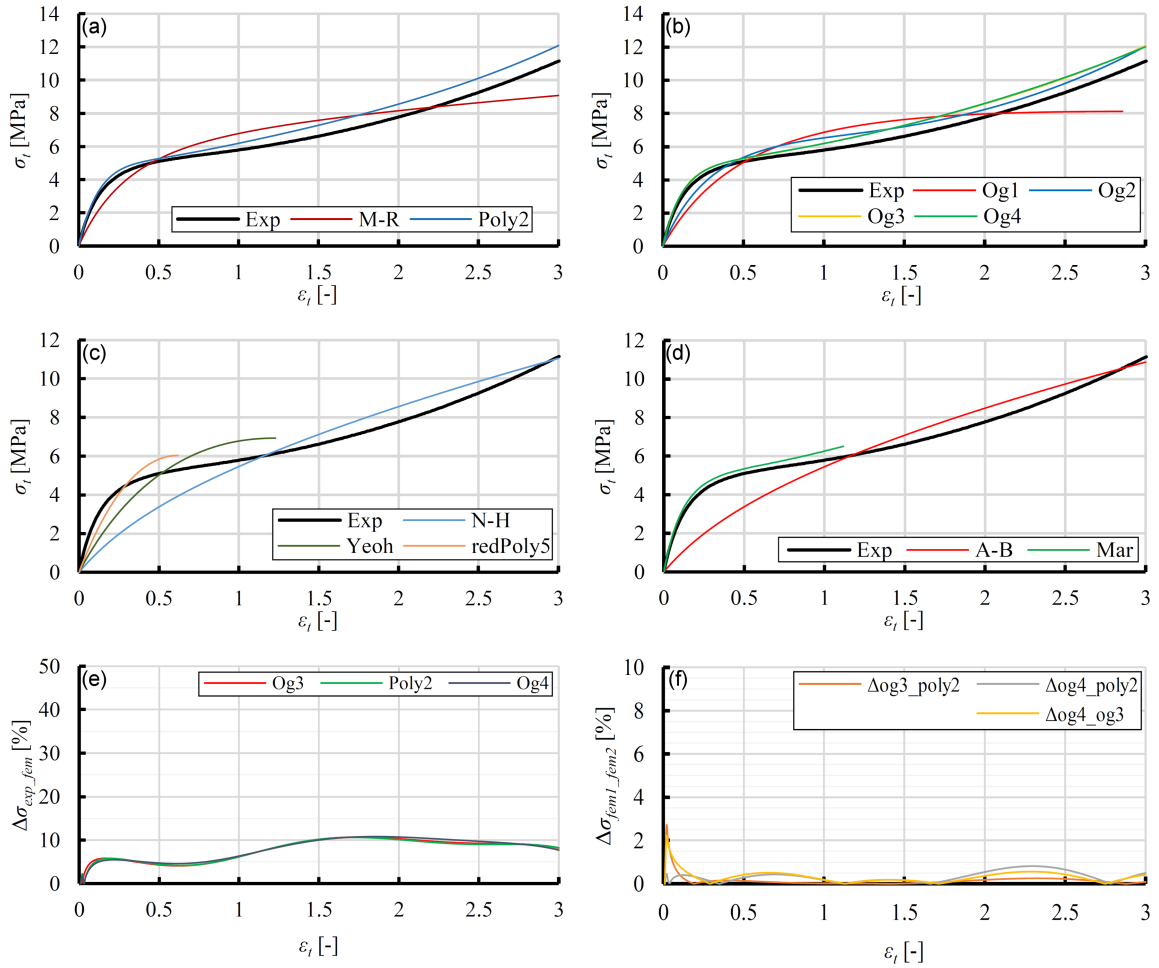

Fig. 3. Results of the second stage of numerical studies. Characteristics $\sigma_t(\varepsilon_t)$ in panels (a–d) show a comparison of the experimental tensile test results (Exp line) at a speed of $v_t = 60$ mm/min with the numerical simulation results for the following models: (a) Mooney–Rivlin (M-R) and 2nd order polynomial (Poly2); (b) 1st order Ogden (Og1), 2nd order Odgen (Og2), 3rd order Ogden (Og3), and 4th order Ogden (Og4); (c) Neo-Hooke (N-H), Yeoh (Yeoh), and reduced 5th order polynomial (redPoly5); (d) Arruda–Boyce (A-B) and Marlow (Mar); (e) Percentage difference function $\Delta\sigma_{exp\_fem}(\varepsilon_t)$ comparing experimental and numerical results; (f) Percentage difference function $\Delta\sigma_{fem1\_fem2}(\varepsilon_t)$ for different numerical models.

model accurately reflects the results of experimental tests. In most practical cases, such a deformation range ($\varepsilon_t < 150\%$) would be sufficient.

In the second stage of the analysis of the results, the difference between the most suitable material models (Og3, Og4, and Poly2) was checked. Using the above-mentioned methodology (see (6)), the percentage difference $\Delta\sigma_{t\_fem1\_fem2}$ between them was determined (Fig. 3f). The difference in the results obtained after the initial section of the tensile curve does not usually exceed 1% (in the initial section of this correlation, it reaches a maximum of $\approx 2.5\%$), which in practice means that these models can be used interchangeably.

Many researchers have addressed the topic of modelling the properties of plastics using models other than hyperelastic ones. Adams et al. [23] dealt with modelling the properties of thermoplastic elastomer (TPE) processed using additive manufacturing technology. The conclusions of this research indicate that in the case of dynamic applications, it is necessary to take viscoelasticity into account in the description of the material model. Feng et al. [24] point out that numerical modelling of elastomers, especially in the range of high deformation values, requires the inclusion of viscosity in the material model due to the possibility of taking into account the influence of deformation speed, which allows for a more precise description of the actual deformation process during simulation. Raj et al. [25], in the conclusions of their work on modelling a composite material with a dominant share of TPU, indicated that the maximum error of the numerical model relative to the experimental results is the smallest for the hyperviscoelastic model, compared to the other models studied, namely hyperelastic and viscoelastic. It should be noted that in the case of these studies, the hyperelastic model

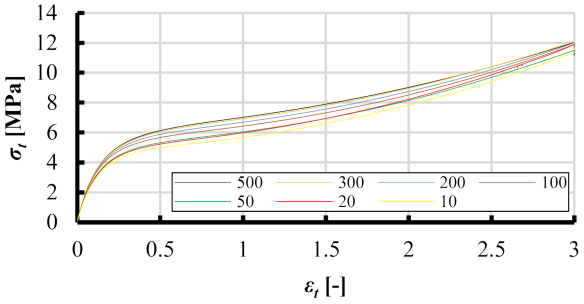

Fig. 4. Results of the second stage of experimental characteristics of tensile stress–tensile strain (σ_t–ε_t), for tests with different tensile speeds v_t = 10, 20, 50, 100, 200, 300, and 500 mm/min.

is characterised by a significantly higher deviation value, which reaches 25%. Given this information, it can be assumed that the maximum numerical model error of 11% (Fig. 3e) may result from the lack of consideration of viscosity, especially given the relatively large deformations applied. Generally, in pure hyperelastic models, the strain rate is not taken into account [22]. Perhaps the use of a model that takes viscosity into account, as well as the introduction of strain rate as another variable, could reduce the model error obtained. In order to verify this hypothesis, a second stage of experimental research was carried out, i.e., a static tensile test with different values of v_t. The results obtained, in the form of $\sigma_t(\varepsilon_t)$ characteristics, are presented in Fig. 4. As can be concluded from them, the strain rate noticeably affects the material's response to displacement. The higher the tensile speed of the sample, the higher the stress value σ_t at the same strain ε_t. Using the same method as in the comparison of experimental and numerical results (see (6)), it was determined that the maximum percentage difference between the stress values for extremely different tensile speeds v_t (10 and 500 mm/min) is $\approx$ 25%, which is a significant value. The nature of the results obtained may indicate that this is due to the viscoelastic character of this material [23–25].

4. Conclusions

As part of two stages of experimental and numerical research, a numerical model was developed to simulate the deformation of TPU C 85 A thermoplastic elastomer under tensile conditions at a constant temperature. Based on the validation of the model with the results of experimental research, the parameters of three hyperelastic material models were obtained, enabling FEM simulation and fairly accurately reproducing the properties of this material under tension, in the range of deformation up to $\approx$ 150%. Based on the results of the second stage of experimental research, it was determined that the deformation speed affects the response of this material to displacement forcing in the tensile range. Taking into account the obtained deviations in the results, the fact that compression of the material occurs during welding, as well as the conclusions from the analysis of the influence of the tensile velocity on the obtained characteristics, the following steps were planned for further numerical research: formulation of a refined simulation model, obtaining parameters of viscoelasticity, and comparison of the results of numerical simulations with the results of experimental compression tests, both assuming hyperelastic and viscoelastic mechanical characteristics.

References

[1] P. Kah, J. Martikainen, *Rev. Adv. Mater. Sci.* **30**, 189 (2012).

[2] J. Tušek, D. Klobčar, *Stroj. Vestn. J. Mech. E.* **50**, 94 (2004).

[3] D.H. Philips, *Welding Engineering: An Introduction*, John Wiley & Sons, Chichester 2016.

[4] V.K. Stokes, *Polym. Eng. Sci.* **29**, 1310 (1989).

[5] D. Grewell, A. Benatar, *Int. Polym. Process* **22**, 43 (2007).

[6] K. Wałęsa, I. Malujda, K. Talaśka, *Acta Mech. Autom.* **12**, 115 (2018).

[7] M. Riahi, K. Kooshayan, M.F. Ghanati, *Polym. Plast. Technol. Eng.* **50**, 907 (2011).

[8] V.K. Stokes, *Polymer* **40**, 6235 (1999).

[9] H. Potente, *Kunststoffe* **2**, 98 (1989).

[10] H. Potente, J. Natrop, *Polym. Eng. Sci.* **29**, 1649 (1989).

[11] H.J. Qi, M.C. Boyce, *Mech. Mater.* **37**, 817 (2005).

[12] A.D. Drozdov, J. de Claville Christiansen, *Int. J. Eng. Sci.* **44**, 205 (2006).

[13] J. Lambert-Diani, C. Rey, *Eur. J. Mech. A Solids* **18**, 1027 (1999).

[14] R. Eberlein, L. Pasieka, D. Rizos, *Adv. Mater. Lett.* **10**, 893 (2019).

[15] J. Wojnowski, Z. Rosłaniec, *Elastomery* **16**, 7 (2012).

[16] Y. Wang, W. Luo, J. Huang, et al., *Macromol. Theory Simul.* **29**, 2000009 (2020).

[17] BEHAbelt, Product Catalogue 2023/2024, BEHAbelt hompage (accessed Aug. 2025).

[18] K. Wałęsa, A. Wrzesińska, M. Dobrosielska, K. Talaśka, D. Wilczyński, *Materials* **14**, 3826 (2021).

[19] ISO 527-2:2025, "Plastics — Determination of Tensile Properties, Part 2: Test Conditions for Moulding and Extrusion Plastics", International Organization for Standardization, Geneva 2025.

[20] K. Wałęsa, I. Malujda, J. Górecki, *IOP Conf. Ser. Mater. Sci. Eng.* **776**, 012107 (2020).

[21] ISO 527-1:2019, "Plastics — Determination of Tensile Properties, Part 1: General Principles", International Organization for Standardization, Geneva 2019.

[22] Dassault Systèmes, Abaqus 2016 Analysis User's Guide, Dassault Systèmes, Providence, 2015.

[23] R. Adams, P. Soe, R. Santiago, M. Robinson, B. Hanna, G. McShane, M. Alves, R. Burek, P. Theobald, *Mater. Des.* **180**, 107917 (2019).

[24] H. Feng, J. Zhou, S. Gao, J. Liying, *Acta Mech.* **232**, 4111 (2021).

[25] G.B. Raj, A. Saludheen, A. Kumar Arumugham-Achari, N. George, T. Chacko, *Mech. Time-Depend. Mater.* **27**, 705 (2022).